

Patterned Growth of Long and Clean Boron Nitride Nanotubes on Substrates

Chee Huei Lee¹, Ming Xie¹, Jiasheng Wang¹, Russell E. Cook², and Yoke Khin Yap¹

¹ Michigan Technological University, Houghton, MI 49931, U.S.A.

² Electron Microscopy Center, Argonne National Laboratory, Argonne, IL 60439, U.S.A.

ABSTRACT

For the first time, patterned growth of boron nitride nanotubes (BNNTs) on Si substrates has been achieved by catalytic chemical vapor deposition (CCVD). Following the boron oxide chemical pathway and our growth vapor trapping approach, high quality and quantity BNNTs can be produced. Effective catalysts have been found to facilitate the growth of BNNTs, while some critical parameters of the synthesis have also been identified to control the quality and density. The success of patterned growth of high quality BNNTs not only explains the roles of the effective catalysts during the synthesis process, but could also be of technologically important for future device fabrication.

INTRODUCTION

Boron nitride nanotubes (BNNTs) have gained more research interest in the recent years due to their interesting properties. BNNTs have almost identical structure to carbon nanotubes (CNTs), in which both are formed by seamless tubular structure with strong sp^2 bonded hexagonal network. On the other hand, unlike their C counterpart, BNNTs possess a wide bandgap of ~5.5 eV, which is almost insensitive to the number of walls, diameters, and chiralities [1]. In addition, BNNTs are good in mechanical properties and thermal conductivity [2, 3]. They are also chemically stable to oxidation up to 1000 °C [4]. Besides, modification of the band gap might be possible via several approaches, such as doping [3, 5], the giant Stark effect [6], and deformation [7]. All these fascinating possibilities make BNNTs potentially useful in deep-UV optoelectronic applications, high-temperatures and high-power electronics, as well as their use as boron carrier in boron neutron capture therapy [8]. BNNTs are also attractive for insulating mechanical and reinforcement applications [9].

Synthesis of BNNTs is challenging compared to that of CNTs due to the needs of much higher growth temperatures and complicated chemistry. This has prevented the applications of BNNTs. By far, BNNTs have been synthesized by various methods, including arc-discharge [10, 11], laser ablation/vaporization [12, 13], BN substitution method from CNT templates [14], chemical vapor deposition (CVD) using borazine [15, 16], induction heating boron oxide CVD (BOCVD) [17, 18], as well as ball milling [19]. Among these synthesis techniques, significant progress has been produced by BOCVD for the mass production of multiwall BNNTs and led to potential applications [12, 13]. Nevertheless, this technique requires an induction furnace with specific design for achieve high growth temperatures (usually >1500 °C) and high temperature gradients. Thus direct growth of BNNTs on Si based substrates is prevented by the BOCVD approach. We previously reported low temperature growth of BNNTs by Plasma Enhanced-Pulse Laser Deposition (PE-PLD) technique [20]. However, the length of the product was still short for

practical applications. We have then devoted our efforts to establish an effective growth technique that enables the growth of long BNNTs by catalytic CVD (CCVD) in a conventional horizontal tube furnaces [21], which is commonly used for the synthesis of CNTs [22], and ZnO nanostructures [23, 24]. This is obtained based on the BOCVD approach and our growth vapor trapping mechanism suggested by the whisker nucleation theory [21]. This CCVD approach also allows pattern growth of BNNTs.

EXPERIMENTAL DETAILS

For direct patterned growth of BNNTs, a TEM copper grid (with square mesh of ~ 100 μm width) was firstly taped onto Si substrates (with or without oxides). 30 nm thick Al_2O_3 film was then deposited on these masked substrates by a pulsed laser deposition (PLD) technique [20], followed by another layer of 10 nm thick MgO film. The TEM grid was later removed after the deposition, giving us a well-defined pattern MgO/ Al_2O_3 films. In the CCVD process (figure 1), substrates with catalyst patterns were placed on the top of the combustion boat, in which B, MgO and FeO precursors (molar ratio of 4:1:1) was filled inside the boat. This setup was loaded inside a closed-end quartz tube in the horizontal tube furnace. The precursors and substrates were then heated up to 1200 $^\circ\text{C}$ with an ammonia flow of 200 to 350 sccms for 1 hr. The substrates were taken out after the furnace was cooled down to room temperature within 4 hrs.

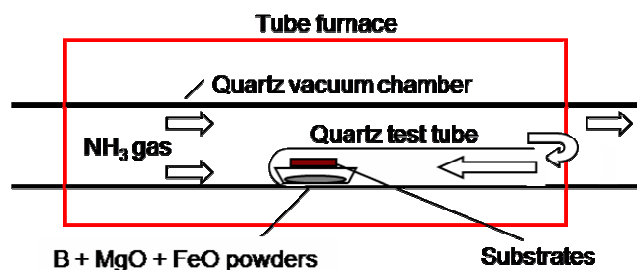


Figure 1. Experimental Setup.

RESULTS AND DISCUSSION

MgO as the Effective Catalyst

In fact, BNNTs could be grown by a spontaneous nucleation from the precursor powders without catalyst films as reported previously [21]. For the CCVD approach described here, we first tested the role of MgO as the catalyst in facilitating the growth of BNNTs. We mixed a small amount of MgO powders in ethanol and dispersed them on Si substrates, followed by the CVD growth. It was found that higher quantity of MgO powders on the substrate produced higher quantity of BNNTs. We note that the size of MgO powders did not affect the diameter of BNNTs significantly as the MgO powder possessed rough surfaces with nano-features, which served as nucleation sites for BNNTs via VLS process [25]. However, more MgO powder catalyst might increase product contamination. Therefore, we further improved our method by depositing MgO thin film using PLD. In the context of control of catalyst contamination, MgO thin film is preferable. Usually, 20 to 30 nm MgO thin films produce the

optimum density, while keeping the catalyst impurity to be the minimum. The quantity of BNNTs on a 2cm x 2cm Si substrate was estimated to be about ~1mg.

Besides, it was found that the amount of precursors could affect the quantity and the diameters of the BNNTs. For comparison, figure 2a indicated the as-grown BNNTs by using amount of precursor powders below the optimum quantity (<0.05g). The average diameter was estimated to be 20 nm to 30 nm. The density of tubes is lower compared to that grown at the optimum condition (figure 2b, ~0.10g). However, by using quantity of precursors higher than the optimum amount (>0.2g), the quality of BNNTs is degraded. As shown in figure 2c, some of the tubes could have diameters >150 nm while the smallest tubes were about 20 nm, and the length of BNNTs were shorter. This situation could be rationalized that more precursors produced more boron oxide source and therefore more quantity of BNNTs formation. Unfortunately, too much growth vapor pressure formed thicker BNNTs walls or even rods. Thus, optimization on the quantity of precursors is needed for the growth of high quality BNNTs. It is not appropriate to control the lengths of BNNTs by simply changing the amount of precursors.

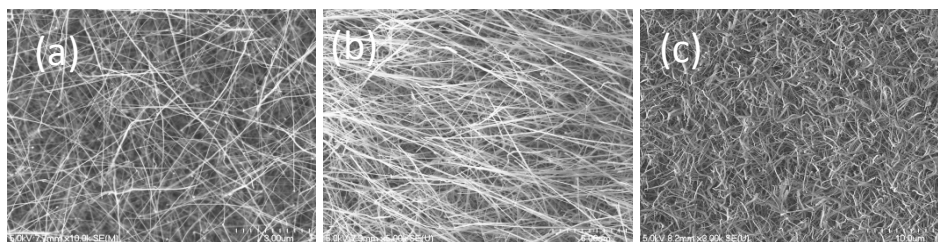


Figure 2. Comparison of different amount of precursors (a) less amount precursor, (b) medium amount precursor, (c) higher amount precursor.

Characterization of BNNTs and Patterned Growth

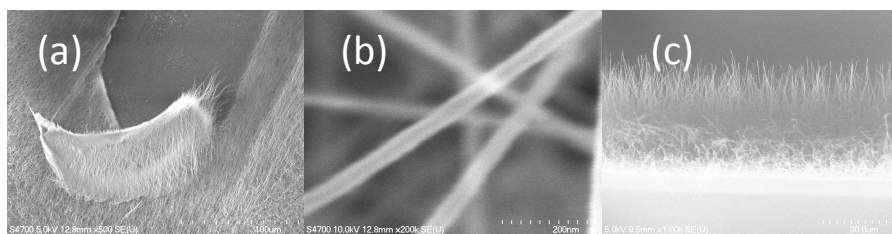


Figure 3. (a) A SEM image of the as-grown BNNTs on a Si substrate. Dense BNNTs can be easily scratched off from a substrate surface. (b) High magnification image reveals the hollow center channel of a tube structure. (c) A cross sectional view of an as-grown sample, indicating a partially vertical aligned morphology.

BNNTs were characterized after optimizing the growth on MgO catalyst films. As indicated from the scanning electron microscopy (SEM) images in figure 3, the typical diameter and length of the tubes were around 20-50 nm and >6 μm , respectively. Besides, these BNNTs could be easily scratched out and collected in an ethanol solution (figure 3a). A magnified SEM image (figure 3b) could reveal the hollow tubular structure of BNNTs. From the cross sectional view of an as-grown sample (figure 3c), these BNNTs were partially vertical aligned on a substrate. It is worth noting that we first observed that this kind of BNNT films exhibited

superhydrophobic property, and thus they may be applicable as self-cleaning and protecting surface [26].

By using patterned MgO/Al₂O₃ films instead of continuous MgO films, BNNTs were found to grow according to the predefined catalyst patterns as shown in figure 4a and 4b. Even though we showed that MgO was the effective catalyst, patterned MgO films alone could not be used for high-quality patterned growth on Si-based substrates (figure 4c). The boundaries of the growth patterns were not well defined in this case. We propose that MgO films tended to diffuse and react with Si to form silicide compounds at high temperatures. This scenario caused the contamination to the non-patterned region (figure 4c). In order to achieve patterned growth, an Al₂O₃ underlayer was needed for growing BNNTs in a well-defined pattern as shown in figure 4a. We think this technique could be technologically important for future applications of BNNTs.

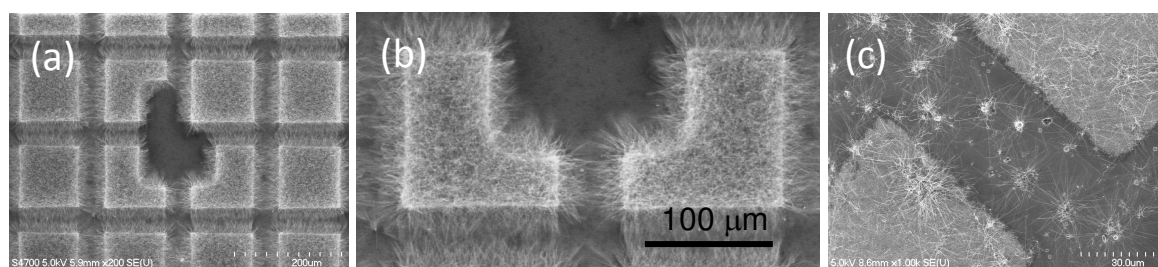


Figure 4. (a) Well defined pattern of BNNTs on a Si substrate with MgO/Al₂O₃ catalyst films by a shadow mask of a copper grid. (b) The magnified view of (a). (c) Growth of BNNTs on patterned MgO films without the Al₂O₃ underlayer. Diffusion of catalysts and contaminations of non-growth regions causes an unsatisfactory patterned growth.

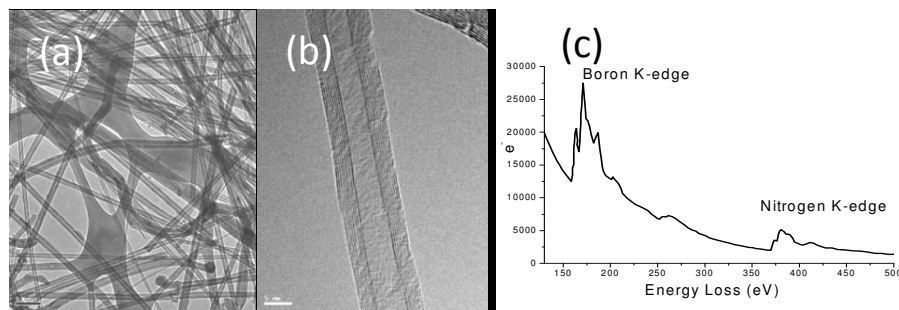


Figure 5. (a) TEM image with a low magnification of bunch of BNNTs. (b) a magnified TEM of a single tube. (c) EELS spectroscopy shows BNNTs with ~1:1 ratio of boron and nitrogen.

High resolution transmission electron microscopy (HRTEM) showed that these BNNTs were highly crystallized, without significant amorphous coatings on the side wall (figure 5a & 5b). Electron Energy Loss Spectroscopy (EELS) indicated that these were pure BNNTs (figure 5c). The lattice vibration of BNNTs was characterized by Raman and Fourier Transformed Infra-red spectroscopy (FTIR). The sharp Raman peak at $\sim 1367\text{cm}^{-1}$ (figure 6a) corresponded to the E_{2g} in-plane vibration mode of the hexagonal BN networks. In FTIR spectra (figure 6b), the $\sim 806\text{cm}^{-1}$ absorption was due to the out-of-plane radial buckling (R) mode. The sharp absorption at $\sim 1368\text{cm}^{-1}$ corresponded to the vibration along the longitudinal (L) or tube axis of a BNNT. We attributed the absorption at $\sim 1523\text{cm}^{-1}$ to the in-plane BN stretching along the tangential (T)

axis of a nanotube. It is noted that this absorption was also predicted by theory, suggesting that this vibration could be the fingerprint for highly crystallized BNNTs [21, 27]. The band gap of these BNNTs was determined to be ~ 6 eV by UV-vis absorption spectroscopy (figure 6c). This band gap is larger than what was recently reported for BNNTs grown by induction heating BOCVD (5.5 V) [28]. For other results and discussion, our detailed findings were recently published in the following reference [29].

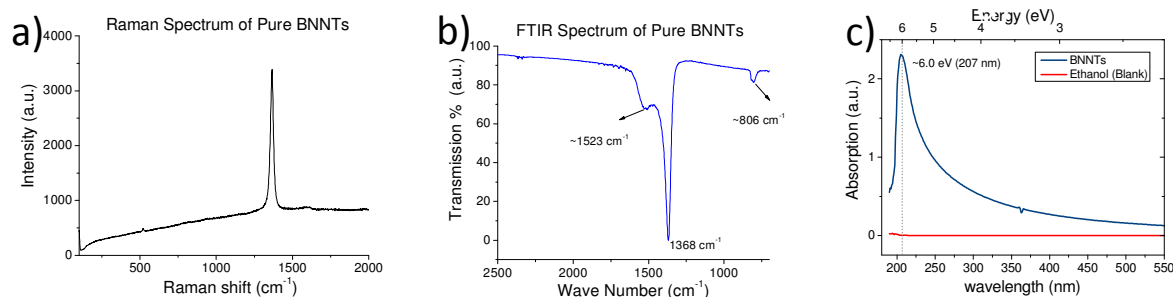


Figure 6. Spectroscopy analysis of pure BNNTs. (a) Raman. (b) FTIR. (c) UV-vis absorption.

CONCLUSION

In summary, we have established a simple CCVD approach for producing high-quality BNNTs. These BNNTs were partially vertical aligned on Si substrates at desired growth location using the patterned MgO/Al₂O₃ catalytic films. The as-grown BNNTs were low in defect level, having a band gap of ~ 6.0 eV without significant sub-band absorption centers. As these BNNTs are grown using a regular tube furnace as for the growth of CNTs and others nanowires, our success has opened a gateway for large scale synthesis and investigation of BNNTs for future applications.

ACKNOWLEDGEMENT

Yoke Khin Yap acknowledges support from the National Science Foundation (*CAREER* Award No. 0447555). Jiasheng Wang is supported by the Department of Energy, the Office of Basic Energy Sciences (Grant No. DE-FG02-06ER46294), and the Electron Microscopy Center at Argonne National Laboratory (Project #080512-01A).

REFERENCES

1. X. Blase, A. Rubio, S. G. Louie, and M. L. Cohen, *Europhys. Lett.* **28**, 335 (1994).
2. N. G. Chopra and A. Zettl, *Solid State Commun.* **105**, 297 (1998).
3. D. Golberg, Y. Bando, C. C. Tang, and C. Y. Zhi, *Adv. Mater.* **19**, 2413 (2007).
4. Y. Chen, J. Zou, S. J. Campbell, and G. L. Caer, *Appl. Phys. Lett.* **84**, 2430 (2004).
5. C. Tang, Y. Bando, Y. Huang, S. Yue, C. Gu, F. Xu, and D. Golberg, *J. Am. Chem. Soc.* **127**, 6552 (2005).

6. M. Ishigami, J. D. Sau, S. Aloni, M. L. Cohen, and A. Zettl, *Phys. Rev. Lett.* **94**, 056804 (2005).
7. X. Bai, D. Golberg, Y. Bando, C. Zhi, C. Tang, M. Mitome, and K. Kurashima, *Nano Lett.* **7**, 632 (2007).
8. G. Ciofani, V. Raffa, A. Menciaci, and A. Cuschieri, *Nanoscale Research Letters* **4**, 113 (2009).
9. Q. Huang, Y. Bando, X. Xu, T. Nishimura, C. Zhi, C. Tang, F. Xu, L. Gao, and D. Golberg, *Nanotechnology* **18**, 485706 (2007).
10. N. G. Chopra, R. J. Luyken, K. Cherrey, V. H. Crespi, M. L. Cohen, S. G. Louie, and A. Zettl, *Science* **269**, 966 (1995).
11. J. Cumings and A. Zettl, *Chem. Phys. Lett.* **316**, 211 (2000).
12. D. P. Yu, et al., *Appl. Phys. Lett.* **72**, 1966 (1998).
13. R. Arenal, O. Stephan, J. L. Cochon, and A. Loiseau, *J. Am. Chem. Soc.* **129**, 16183 (2007).
14. W. Han, Y. Bando, K. Kurashima, and T. Sato, *Appl. Phys. Lett.* **73**, 3085 (1998).
15. O. R. Lourie, C. R. Jones, B. M. Bartlett, P. C. Gibbons, R. S. Ruoff, and W. E. Buhro, *Chem. Mater.* **12**, 1808 (2000).
16. M. J. Kim, S. Chatterjee, S. M. Kim, E. A. Stach, M. G. Bradley, M. J. Pender, L. G. Sneddon, and B. Maruyama, *Nano Lett.* **8**, 3298 (2008).
17. C. Tang, Y. Bando, T. Sato, and K. Kurashima, *Chem. Commun.* 1290 (2002).
18. C. Zhi, Y. Bando, C. Tan, and D. Golberg, *Solid State Commun.* **135**, 67 (2005).
19. H. Chen, Y. Chen, Y. Liu, L. Fu, C. Huang, and D. Llewellyn, *Chem. Phys. Lett.* **463**, 130 (2008).
20. J. Wang, V. K. Kayastha, Y. K. Yap, Z. Fan, J. G. Lu, Z. Pan, I. N. Ivanov, A. A. Puzos, and D. B. Geohegan, *Nano Lett.* **5**, 2528 (2005).
21. C. H. Lee, J. Wang, V. K. Kayastha, J. Y. Huang, and Y. K. Yap, *Nanotechnology* **19**, 455605 (2008).
22. V. K. Kayastha, S. Wu, J. Moscatello, and Y. K. Yap, *J. Phys. Chem. C* **111**, 10158 (2007).
23. S. L. Mensah, V. K. Kayastha, and Y. K. Yap, *J. Phys. Chem. C* **111**, 16092 (2007).
24. S. L. Mensah, V. K. Kayastha, I. N. Ivanov, D. B. Geohegan, and Y. K. Yap, *Appl. Phys. Lett.* **90**, 113108 (2007).
25. A. W. Brent, A. D. Kimberly, J. Jonas, T. B. Magnus, D. Knut, and S. Lars, *Adv. Mater.* **21**, 153 (2009).
26. C. H. Lee, J. Drelich, and Y. K. Yap, *Langmuir* **25**, 4853 (2009).
27. L. Wirtz, A. Rubio, R. A. de la Concha, and A. Loiseau, *Phys. Rev. B* **68**, 045425 (2003).
28. P. Jaffrennou, J. Barjon, J. S. Lauret, A. Maguer, D. Golberg, B. Attal-Trétout, F. Ducastelle, and A. Loiseau, *phys. stat. sol. (b)* **244**, 4147 (2007).
29. C. H. Lee, M. Xie, V. Kayastha, J. Wang and Y. K. Yap, *Chem. Mater.*, Articles ASAP (DOI: 10.1021/cm903287u). (URL: <http://pubs.acs.org/doi/full/10.1021/cm903287u>)